www.ijbar.org
ISSN 2249-3352 (P) 2278-0505 (E)
Cosmos Impact Factor-5.86

Grid-Interfaced Electric Vehicle Charging Stations Using a Fuzzy Logic-Based Approach

Sayed Raziya Sultana[1], Pillalamarri Yamini Lakshmi[2], Metra Rama Koteswara Naga Babu[3], Yaddanapudi Jaya Prakash[4], Dr.N.Chaitanya[5]
1,2,3,4 UG Students, Department of Electrical and Electronics Engineering
5,Associate Professor,M.Tech,Ph.D,,Department of Electrical and Electronics Engineering
R.V.R&J.C College of Engineering , Chowdavaram,Guntur, Andhra Pradesh 522019,India.
sayed.raziyasultana1313@gmail.com, pyaminilakshmi6@gmail.com, mrknagababu2003@gmail.com , yaddanapudiprakash272@gmail.com, nc@rvrjc.ac.in

ABSTRACT

This research paper proposes a novel grid-connected modular inverter for an integrated bidirectional charging station designed for residential applications. The system enhances grid stability by providing buffering services and supporting energy management. It consists of a modular bidirectional inverter that functions as an electric vehicle (EV) charger, operating in multiple modes, including EV battery charging and discharging, storing excess grid energy during low-demand periods, and supplying energy back to the grid during peak demand. To optimize power flow between the EV battery, household load, and the grid, a low-level control strategy based on the droop control technique and feedforward decoupling is implemented, replacing the conventional PI controller with a fuzzy logic controller (FLC). The use of FLC improves system adaptability, dynamic response, and robustness against parameter variations. The system's performance is evaluated through MATLAB/Simulink simulations, demonstrating its ability to support the grid during peak demand and enhance renewable energy integration. Additionally, it provides backup power during outages, increasing overall reliability.

Key words: Bidirectional control, DC charging station, droop control, VSI, V2G and V2H.

I. Introduction

The increasing integration of electric vehicles (EVs) into residential applications necessitates the development of efficient and sustainable charging solutions. Existing research has explored various charging methodologies, particularly focusing on bidirectional charging stations that enable Vehicle-to-Grid (V2G) and Vehicle-to-Home (V2H) functionalities. The literature highlights the need for modular inverters to enhance energy management and grid stability while ensuring optimal power flow between the EV battery, household loads, and the power grid.

Bidirectional Charging and Energy Management

Bidirectional charging technology plays a crucial role in energy buffering and grid support. Several studies emphasize that EV batteries can store excess energy during low-demand periods and discharge it back to the grid during peak hours. This technology enhances energy utilization efficiency, reduces dependency on conventional energy sources, and provides a potential revenue stream for EV owners through grid energy resale [1]. The use of a modular inverter in bidirectional charging stations further improves system reliability by allowing adaptive power flow management and voltage regulation [2].

Control Strategies for Smart Charging

Various control strategies have been proposed to manage energy exchange between EVs and the grid. The conventional proportional-integral (PI) controller is widely used in energy management systems; however, its limitations in dynamic adaptability necessitate alternative approaches. Recent studies indicate that replacing PI controllers with fuzzy logic controllers (FLC) improves system robustness and adaptability under varying grid conditions. FLC enables efficient energy distribution and enhances voltage stability by dynamically adjusting power flow parameters [3]. Additionally, droop control techniques and feedforward decoupling have been explored to optimize power flow and minimize disruptions in grid operations [4].

Renewable Energy Integration with EV Charging

The integration of Renewable Energy Sources (RES) with EV charging stations has gained significant attention. Solar photovoltaic (PV) systems are commonly used in residential energy setups, contributing to decentralized power generation. Research indicates that solar energy's share in power production is expected to increase from 33% to 67% by 2030, with a substantial portion coming from rooftop installations [5]. Combining RES with bidirectional charging infrastructure can further enhance sustainability by reducing reliance on grid electricity and enabling self-sufficient energy management [6].

Communication Protocols and System Interoperability

An essential aspect of bidirectional charging systems is the implementation of standardized communication protocols to ensure seamless operation. The ISO 15118-20 protocol facilitates secure and efficient data exchange between EVs and charging stations, allowing real-time energy flow management. Power Line Communication (PLC) has been identified as a viable method for extracting EV battery information and enabling smart charging operations [7]. Studies have also examined the CHAdeMO and Combo CCS Type 2 connectors for bidirectional energy transfer, highlighting their potential in enhancing the practicality of V2G and V2H applications [8].

Economic Feasibility and Cost Considerations

Economic assessments of DC charging infrastructure suggest that integrating bidirectional charging with residential energy management systems can significantly reduce the Total Cost of Ownership (TCO). Recent studies indicate that such systems can lead to a 30% reduction in operational costs for EV charging network operators while providing financial benefits to homeowners through reduced grid dependency and optimized energy consumption [9]. However, challenges such as infrastructure costs and policy limitations still need to be addressed to facilitate widespread adoption [10].

The reviewed literature underscores the importance of developing an efficient and adaptive bidirectional charging system for residential applications. Modular inverter technology, coupled with advanced control strategies such as fuzzy logic controllers and droop control techniques, enhances system performance and energy efficiency. Furthermore, integrating RES and implementing robust communication protocols can further optimize the functionality of V2G and V2H systems. Future research should focus on addressing infrastructure challenges and refining economic models to promote the large-scale deployment of sustainable EV charging solutions.

II. Grid integrated DC Charging Station

A conventional household power generation system is illustrated in Figure 1. At the core of this system is a 10 kW grid-tied inverter, which supplies AC power from a 10 kWp solar PV array to both the household loads and an electric vehicle (EV) wall box charger [18], [19]. The average monthly electricity consumption for a typical four-person household in Belgium is considered to be 20 kWh [20]. To ensure two days of energy autonomy, the required battery energy storage system (BESS) size is estimated at 66 kWh.

The wall box charger provides AC power to the EV through an on-board charger (OBC), supporting a charging capacity of up to 7.4 kW, suitable for private garage use. For instance, charging a Volkswagen ID Buzz with a 77 kWh battery and 350 V battery voltage takes approximately 10.5 hours. However, the wall box does not support Vehicle-to-Grid (V2G) services due to the unidirectional nature of conventional OBCs. Furthermore, the AC wall box typically uses the OCPP 1.6j protocol, which lacks support for bidirectional power flow, and is not compatible with smart charging or Vehicle-to-Home (V2H) applications when integrated with solar PV and BESS.

These limitations can be overcome by upgrading to a bidirectional DC charging system integrated with a grid-tied inverter, using a Combo CCS Type 2 port. The enhanced system architecture is presented in Figure 2.

The proposed solution supports bidirectional DC charging up to 22 kW and enables V2G services at home. Additionally, the EV battery can serve as an energy buffer during emergencies or for evening power backup. During sunny summer days, the solar PV can meet household demand, charge the BESS, or export excess energy to the grid if the BESS is full. With the proposed setup, solar energy can also be stored in EVs and home batteries during the day, then discharged to power household loads in the evening, allowing for a reduction in the required BESS capacity compared to traditional sizing methods [18].

The system's operation mode is dynamically adjusted based on solar irradiance, the state-of-charge (SoC) of both the EV and the BESS, and real-time electricity pricing. These modes are illustrated in Figure 3:

www.ijbar.org
ISSN 2249-3352 (P) 2278-0505 (E)
Cosmos Impact Factor-5.86

Activation of V2G mode typically depends on grid conditions such as voltage and frequency fluctuations, and requires the homeowner's consent. In this mode, the system operates in grid-connected mode to export energy from the EV battery back to the grid.

III. Proposed system and its control strategy design

The proposed bidirectional EV charging station with integrated buffered BESS support, as described in Section II, operates in multiple modes to enable flexible and efficient power flow. It is designed to support bidirectional power transfer depending on the operational requirements. When drawing power from the EV battery, the system can function in two distinct modes:

1. Standalone Mode (Grid-Forming):

In this mode, the EV battery supplies power directly to household loads during emergencies, as illustrated in Figure 1(a). The converter operates independently of the grid, maintaining a constant output voltage and frequency. Since the inverter defines the frequency rather than following the grid, this is referred to as grid-forming mode.

2. Grid-Connected Mode (Charging and Discharging):

When the EV is charging or discharging while connected to the grid, the converter operates in grid-following mode, as shown in Figure 1(b). During charging, the AC/DC converter regulates its output voltage in response to the grid's input to deliver controlled power to the EV battery. In discharging or V2G (Vehicle-to-Grid) operation, the DC/AC converter inverts the battery's DC power into AC and feeds it back into the grid. To ensure proper synchronization, the inverter matches its voltage and frequency to those of the grid.

The control strategies for different operational modes—including charging, V2G, and V2H (Vehicle-to-Home)—are discussed in the following subsections. The charging station architecture consists of multiple AC/DC converter modules connected in parallel, enabling modular operation and scalability.

In this mode, the system actively interacts with the power grid to either absorb energy for charging the electric vehicle battery or supply energy back when required. It uses synchronized control to ensure smooth power exchange, maintaining voltage and frequency within grid standards. The energy flow is managed intelligently based on real-time factors like battery charge level, household consumption, and grid demands. During charging, the system ensures stable voltage regulation, while in discharging mode, it supports the grid by injecting power in a controlled manner. Advanced control techniques, including fuzzy logic, enhance responsiveness and stability, especially under fluctuating load conditions. This dual capability not only optimizes energy usage but also contributes to grid reliability and flexibility.

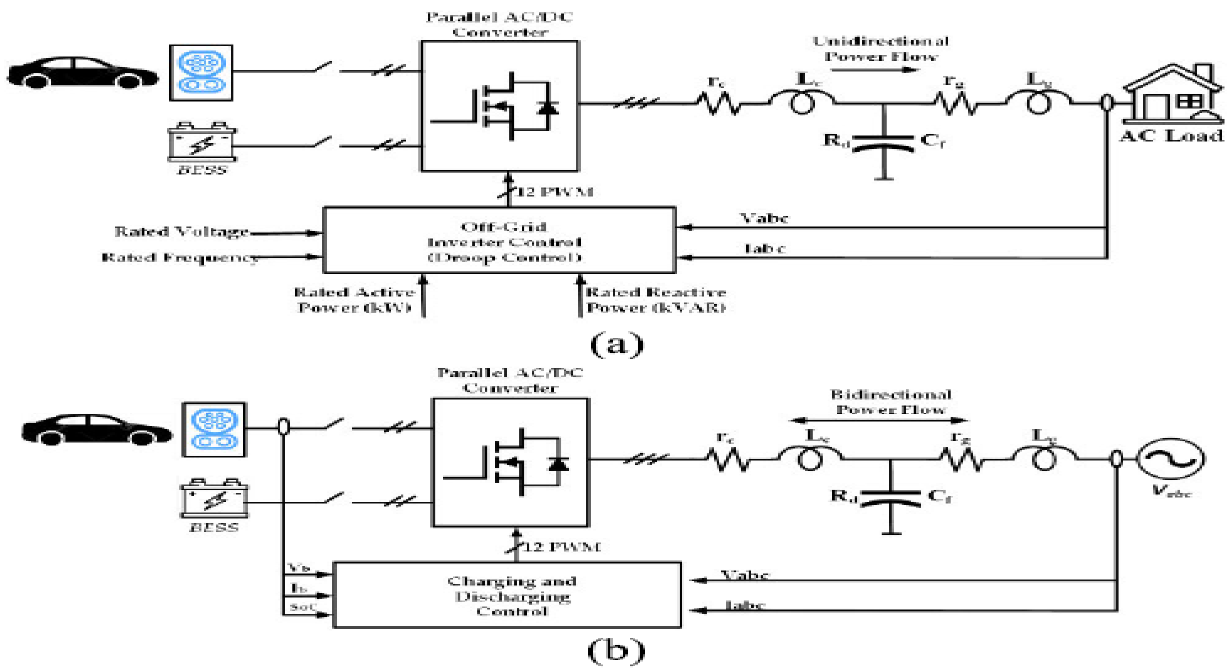

FIGURE 1. Proposed integrated charging station converter control strategies. (a) Off-grid inverter control for V2H mode; (b) Charging and discharging control for charging G2V and V2G mode.

A. OFF-GRID INVERTER MODE (V2H MODE)

In the off-grid (Vehicle-to-Home or V2H) mode, the inverter operates in grid-forming control mode to generate a constant three-phase voltage with fixed magnitude and frequency [23]. This mode is active when the house is disconnected from the main utility grid, meaning the inverter supplies power to the local load using renewable energy sources or energy storage systems.

Figure 2 illustrates the complete standalone control scheme for the grid-connected inverter operating in off-grid mode. The control system features a dual-loop structure, comprising both current and voltage control loops, and includes a phase-locked loop (PLL) for synchronizing with external three-phase signals via dq-axis transformation.

$$f_{ref} = f_0 - K_p(P - P_0)$$
$$V_{ref} = V_0 - K_q(Q - Q_0)$$
$$P = v_d i_d + v_q i_q$$
$$Q = v_d i_q + v_q i_d$$

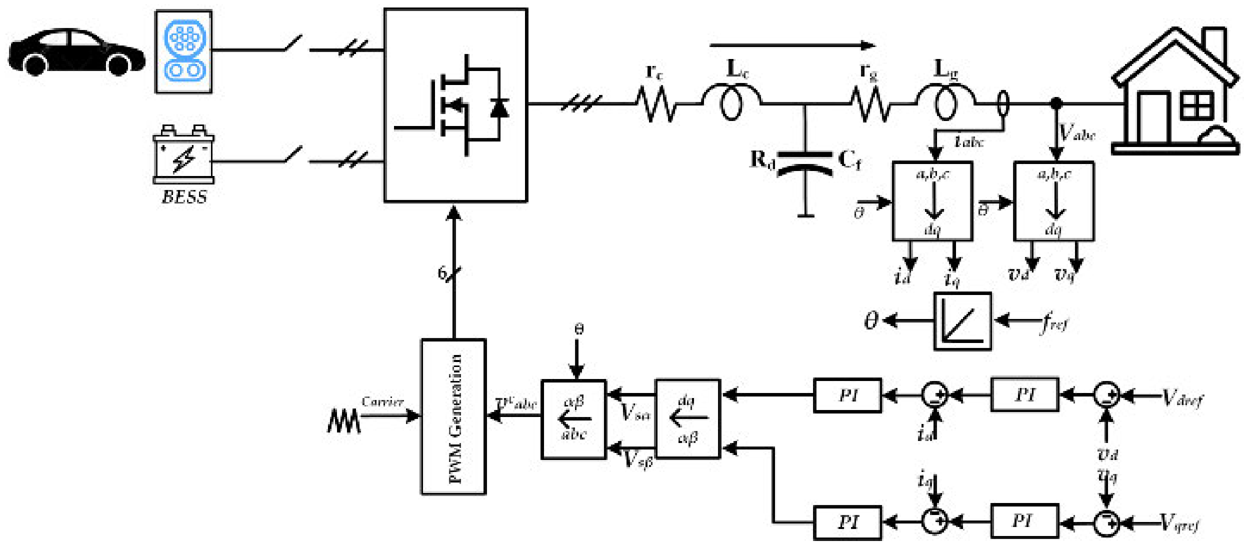

FIGURE 2. Off-grid inverter control to maintain the voltage and frequency of the household load.

B. EV CHARGING MODE (G2V MODE)

In Grid-to-Vehicle (G2V) mode, the power converter functions as a rectifier, enabling energy transfer from the three-phase grid to the electric vehicle (EV) battery. A dual-loop feedforward decoupling control strategy is employed [24], consisting of an outer voltage control loop and an inner current control loop for managing the d-axis and q-axis currents, as illustrated in Figure 3.

The inner current loop operates at a higher speed and is responsible for controlling the current through the active front end by generating appropriate control signals (duty cycles). This fast response loop ensures quick adaptation to load current variations and helps minimize current harmonics.

$$v_d^c = e_d + \omega L_g i_q - (K_p + \frac{K_i}{s})(i_{dref} - i_d)$$
$$v_q^c = e_q + \omega L_g i_d - (K_p + \frac{K_i}{s})(i_{qref} - i_q)$$

ISSN 2249-3352 (P) 2278-0505 (E)
Cosmos Impact Factor-5.86

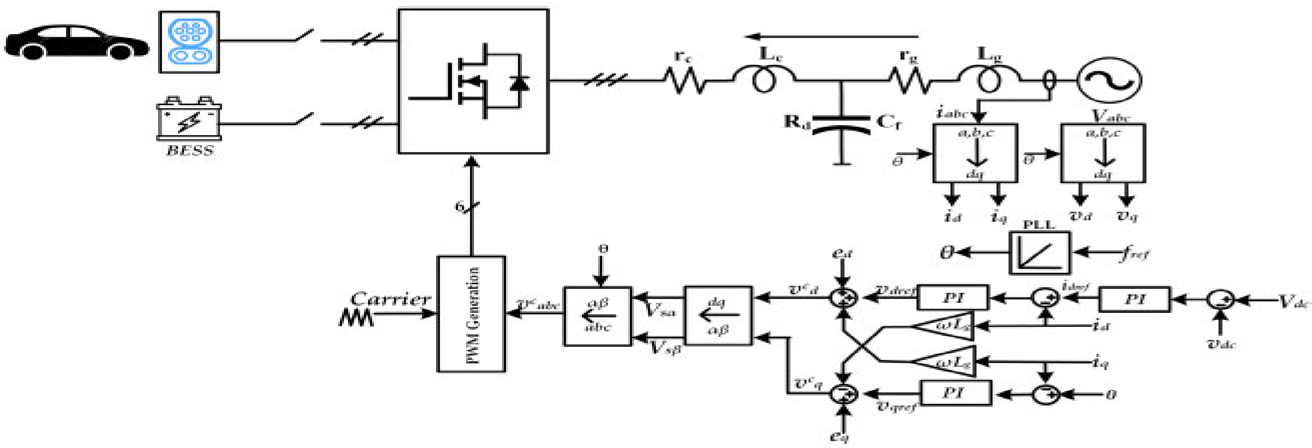

FIGURE 3. EV battery charging control via feedforwarding decoupling strategy.

C. EV Battery Discharging Mode (V2G Mode)

In the Vehicle-to-Grid (V2G) mode, the inverter adjusts the active and reactive power it injects based on the main grid's voltage and frequency, as illustrated in Figure 4. The inverter determines the required currents using equations (20) and (21), where K_P and K_Q represent the droop control parameters, and K′_P and K′_i are the proportional-integral (PI) controller gains, which enhance the quality of the injected power. When the grid operates at its nominal voltage and frequency—400V and 50 Hz—the inverter delivers the rated active and reactive power. In the event of any deviation from these nominal values, the inverter dynamically adjusts the power output to support grid stability, as described in [19].

$$I_{d\_bias} = \left[(P - P_0) - \frac{1}{K_P}(f - f_0)\right]\left[K'_{pp} + \frac{K'_{ip}}{s}\right]$$

$$I_{q\_bias} = \left[(Q - Q_0) - \frac{1}{K_Q}(V - V_0)\right]\left[K'_{pp} + \frac{K'_{ip}}{s}\right]$$

www.ijbar.org
ISSN 2249-3352 (P) 2278-0505 (E)
Cosmos Impact Factor-5.86

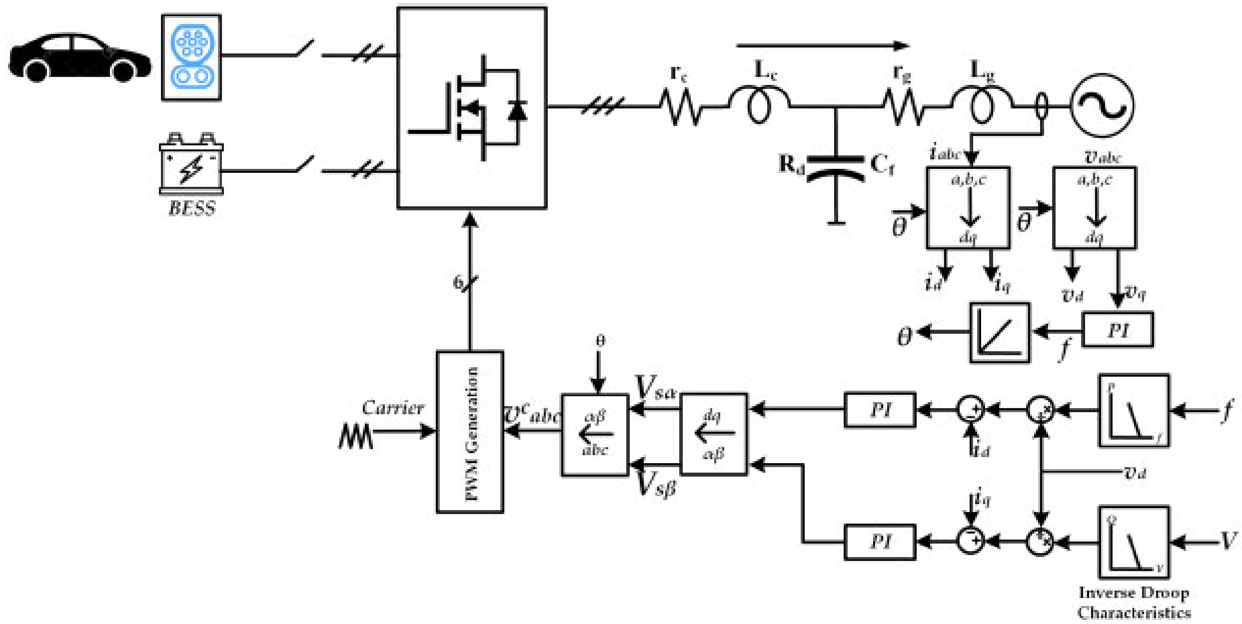

FIGURE 4. EV battery discharging control by grid-following droop control strategy to maintain grid voltage and frequency.

D. Operating Mode Control Strategy

Ongoing research is focused on developing a comprehensive energy management strategy and evaluating the total cost of ownership (TCO) for the proposed system.

The process begins by retrieving key EV parameters, including the battery state of charge (SoC), battery voltage (V_b), arrival time (T_a), and departure time (T_d). If the current SoC falls below a predefined minimum threshold (SoC_{min}), which ensures a sufficient charge for emergency use, the system initiates the grid-to-vehicle (G2V) mode. In this mode, the EV battery is charged using a constant current–constant voltage (CC-CV) method. Charging continues until the SoC reaches SoC_{max}, typically around 80% of full capacity.

The vehicle-to-grid (V2G) mode is activated under two specific conditions: the SoC must be equal to or greater than SoC_{max}, and the EV owner must grant permission for V2G operation. Similarly, activation of the vehicle-to-home (V2H) mode also requires explicit consent from the EV user.

IV. Simulation result:

1. Simulation results for Standalone Mode:

www.ijbar.org
ISSN 2249-3352 (P) 2278-0505 (E)
Cosmos Impact Factor-5.86

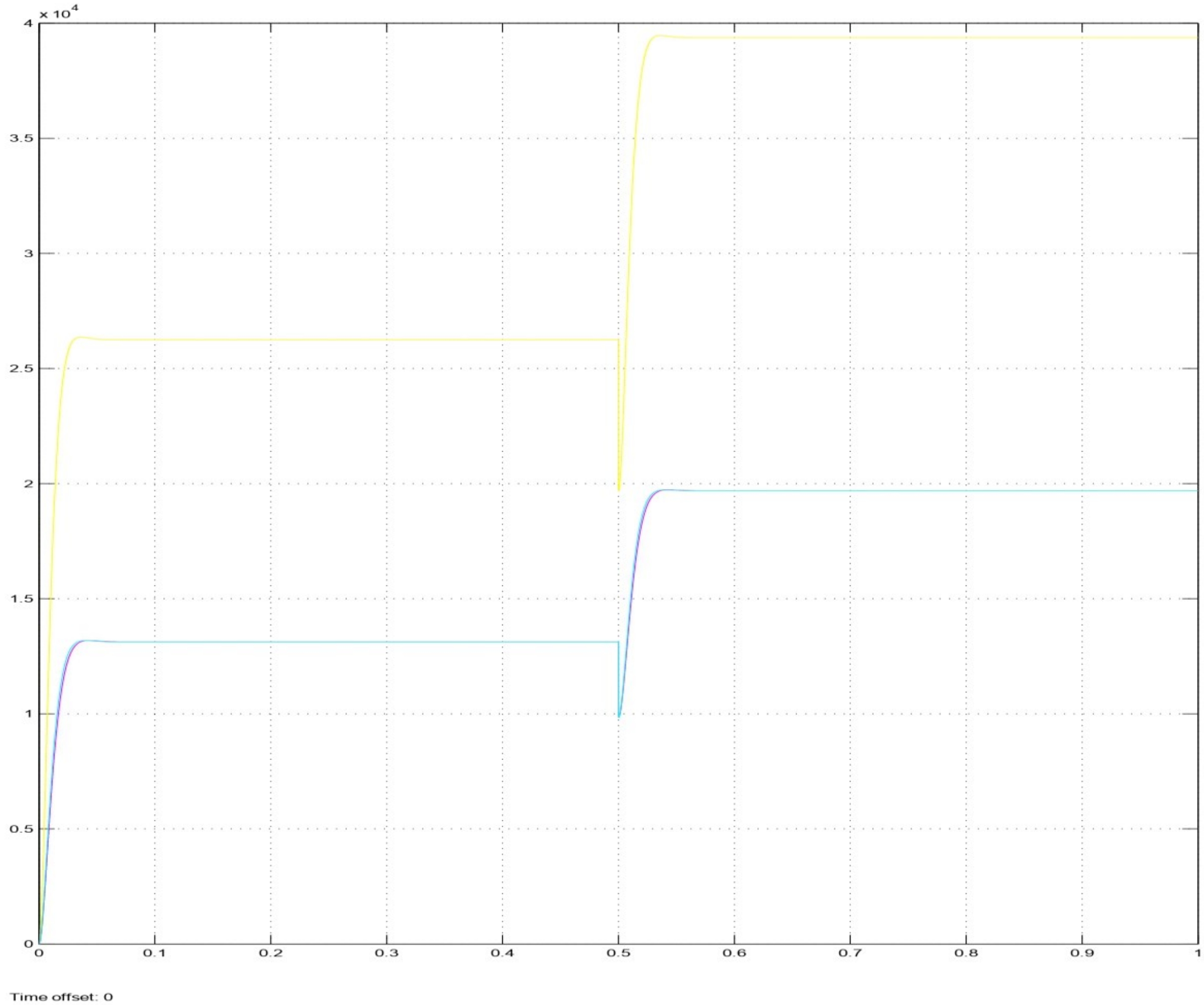

Fig.5(a)

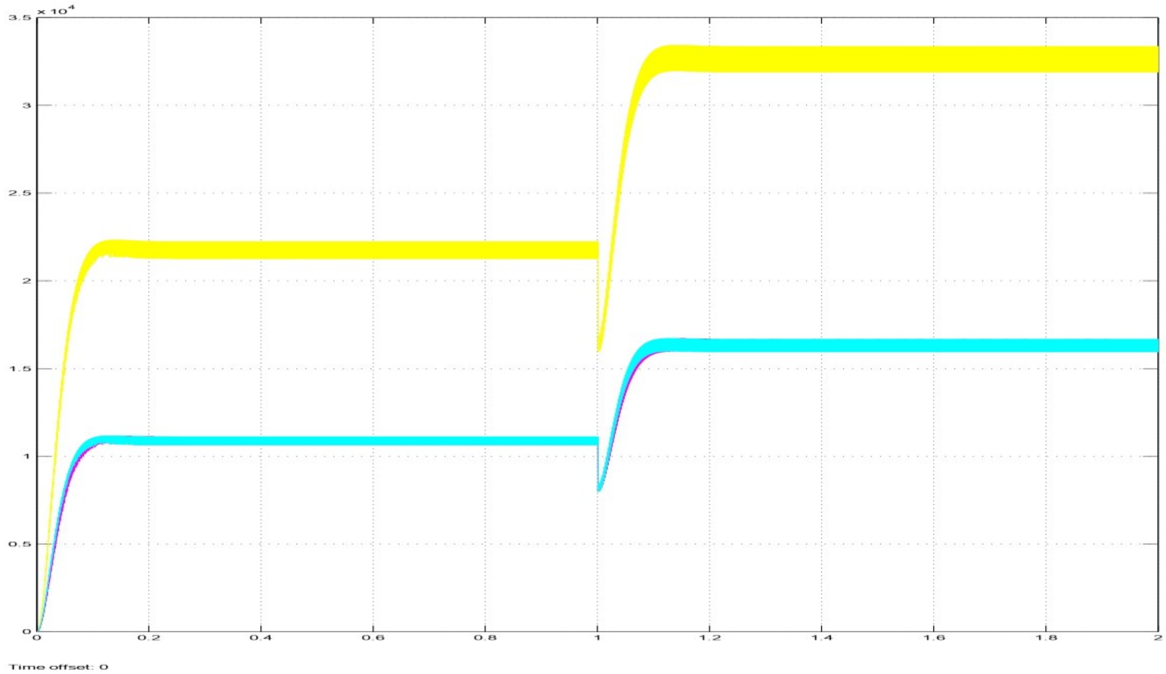

Fig.5(b)

Fig.5 Variation of Reactive Power with Load Disturbance in Standalone Mode

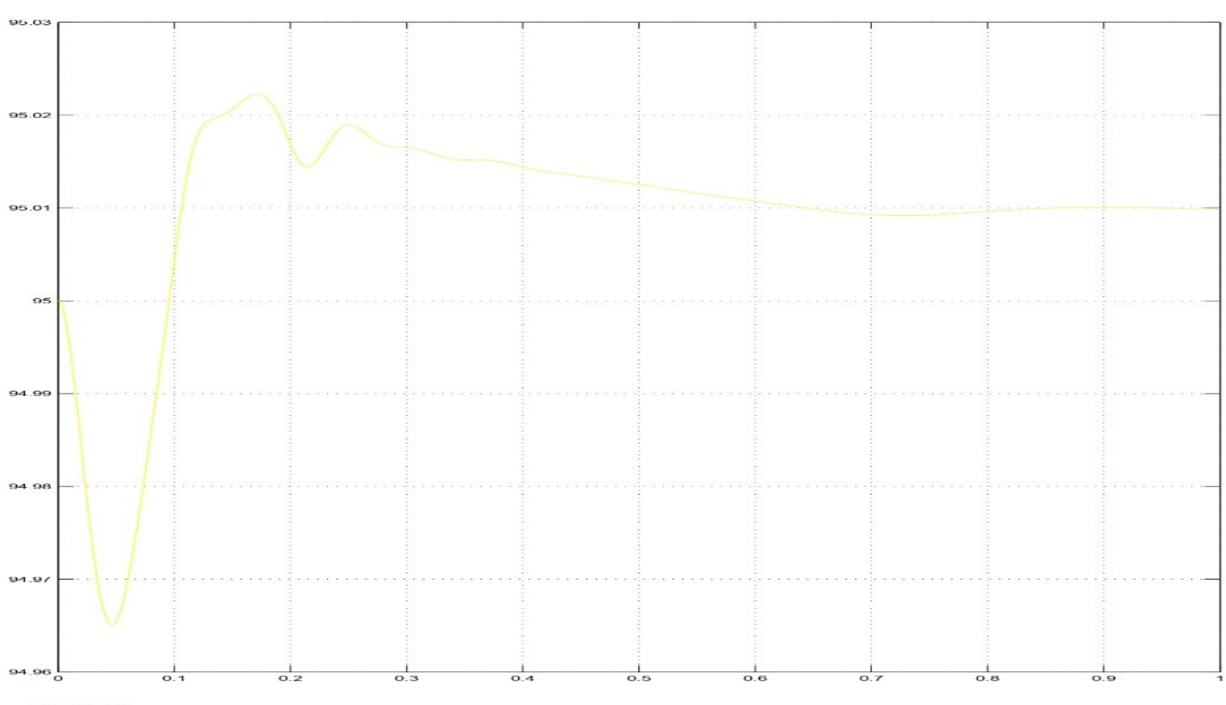

Fig.6 State of Charge (SoC) Variation of EV Battery in Standalone Mode

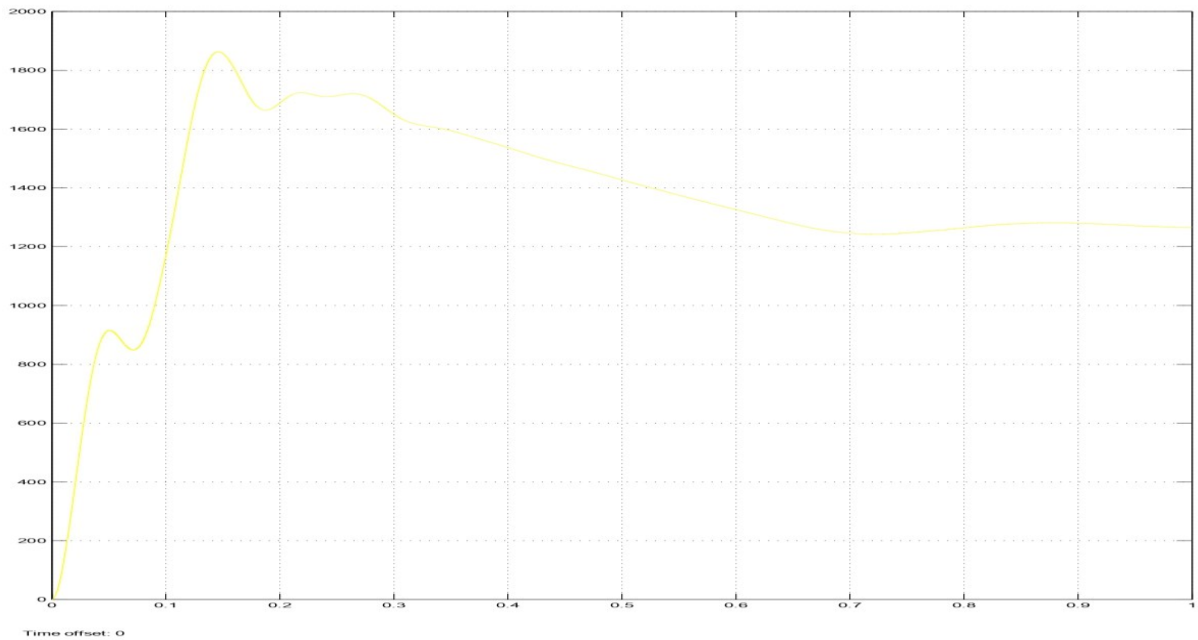

Fig.7 DC-Link Voltage Stability During Converter Operation in Standalone Mode

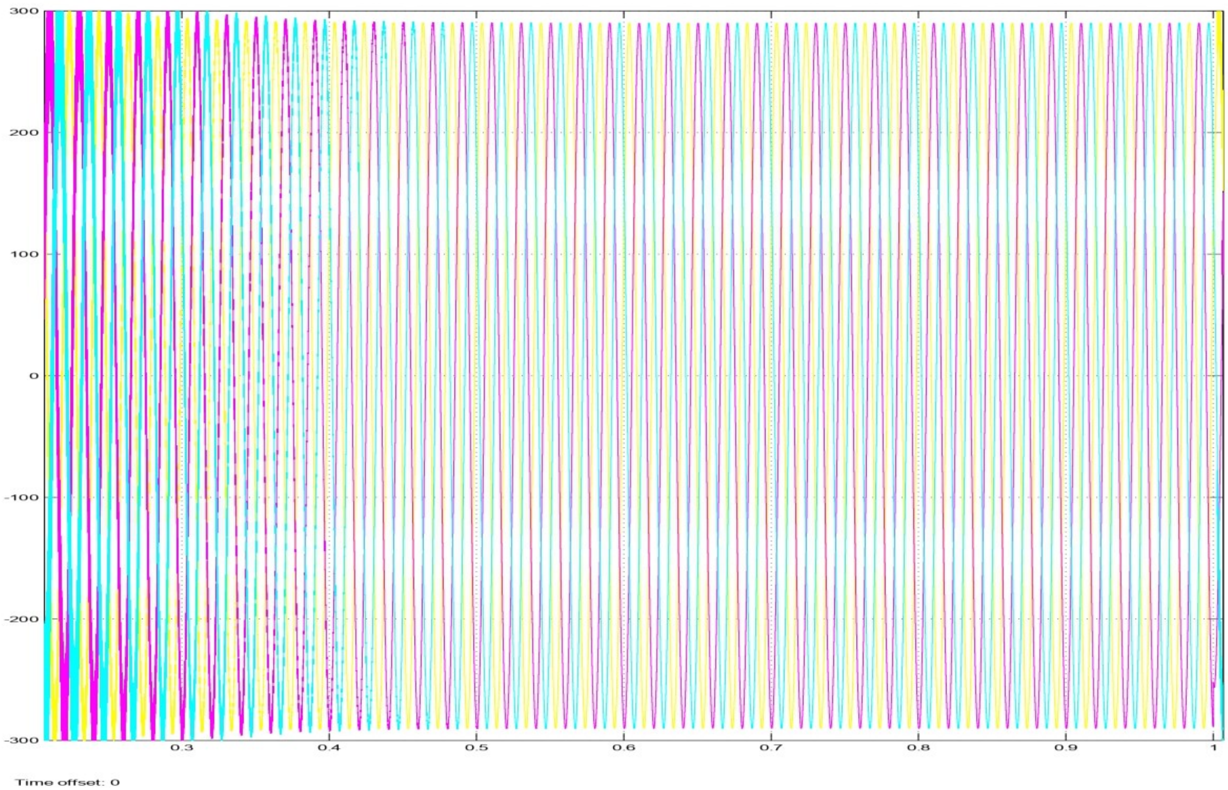

Fig.8 Grid Voltage Response During V2G Operation

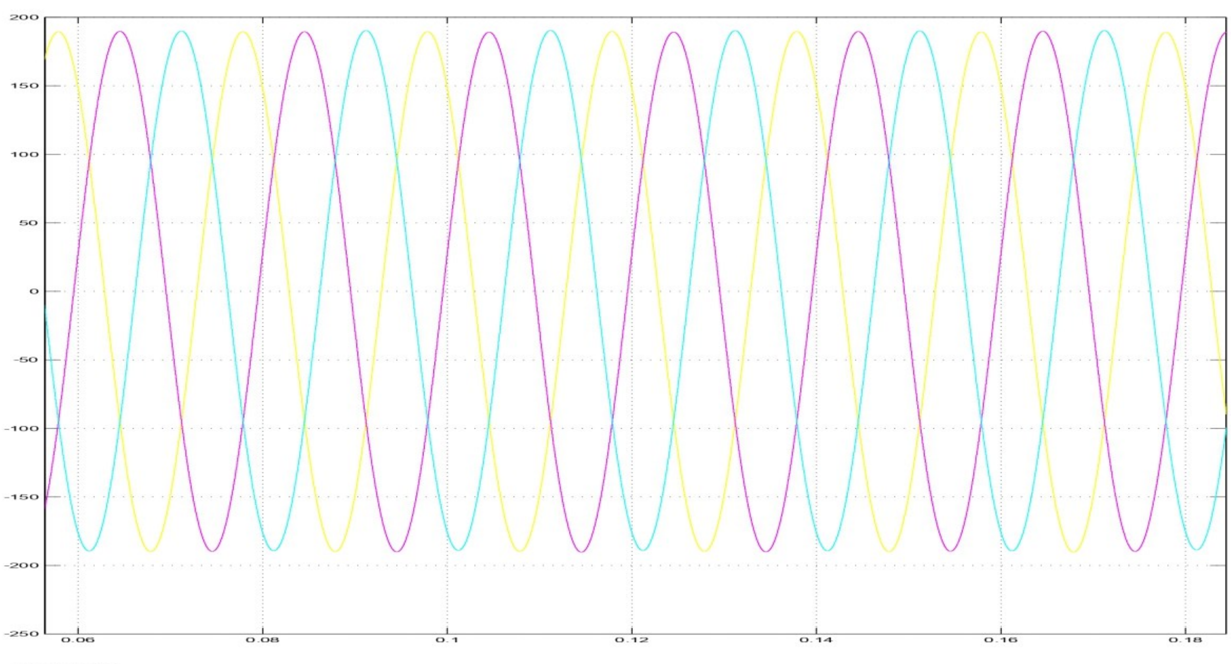

Fig.9 Grid Current Response During Charging and V2G Mode

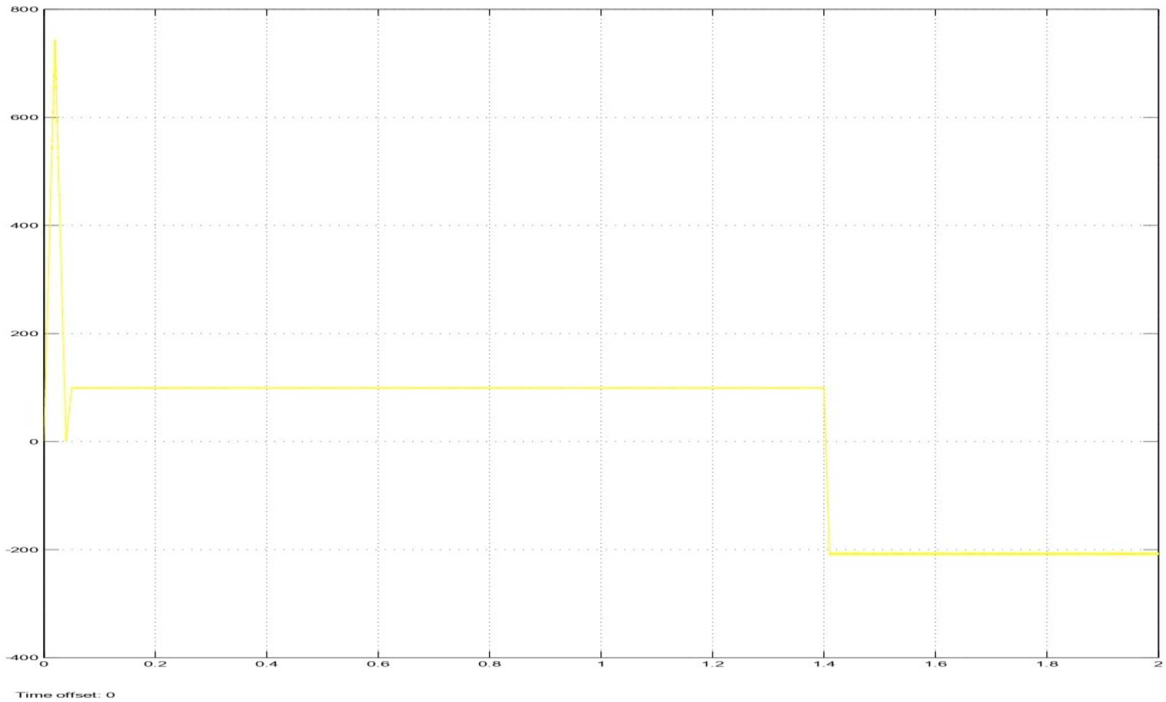

Fig.10 Battery Voltage Profile Under Varying Load Conditions

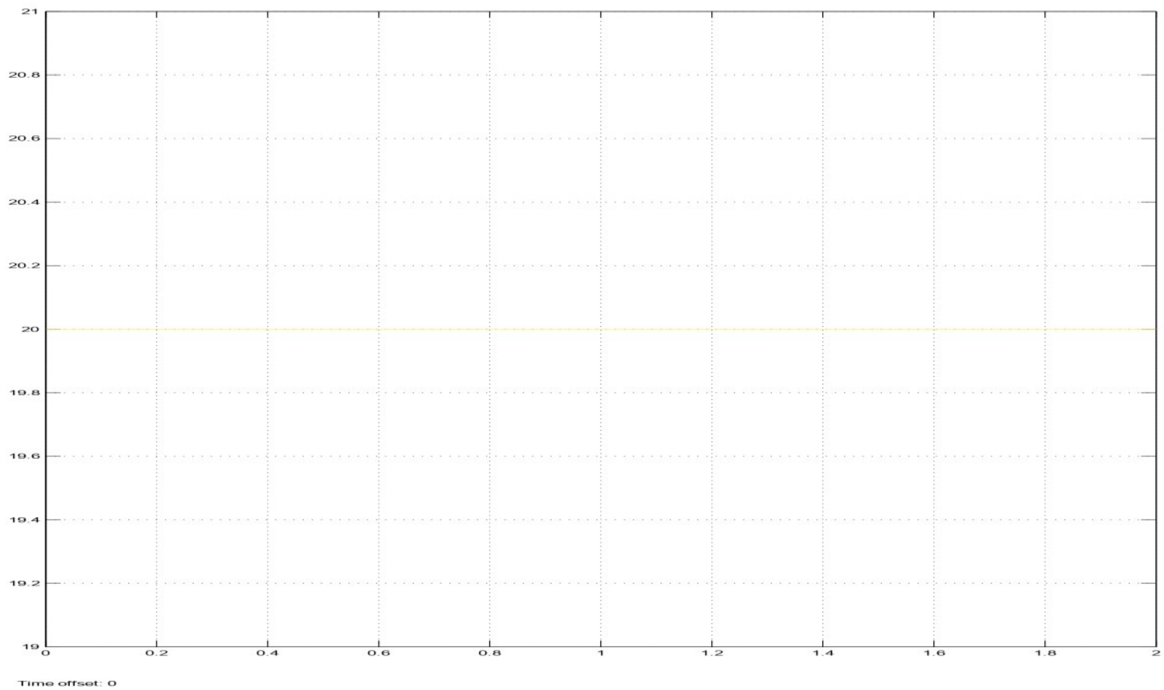

Fig.11 EV Battery Current Response During Bidirectional Operation

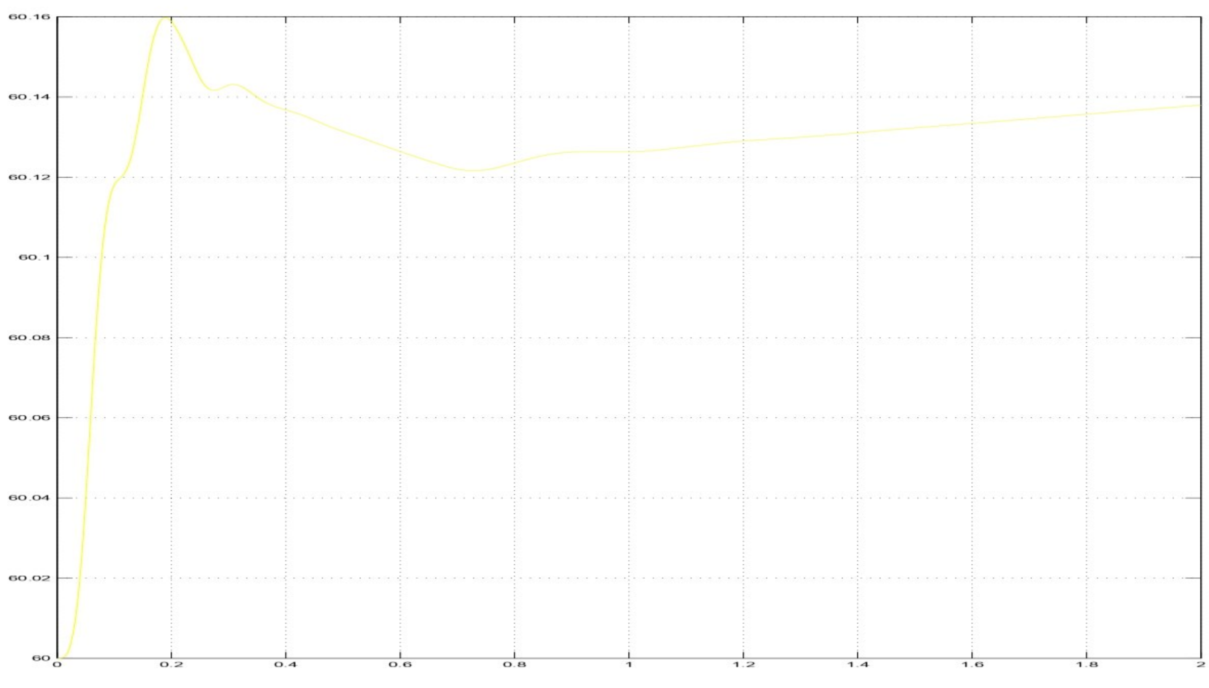

Fig.12 State of Charge (SoC) Variation of EV Battery

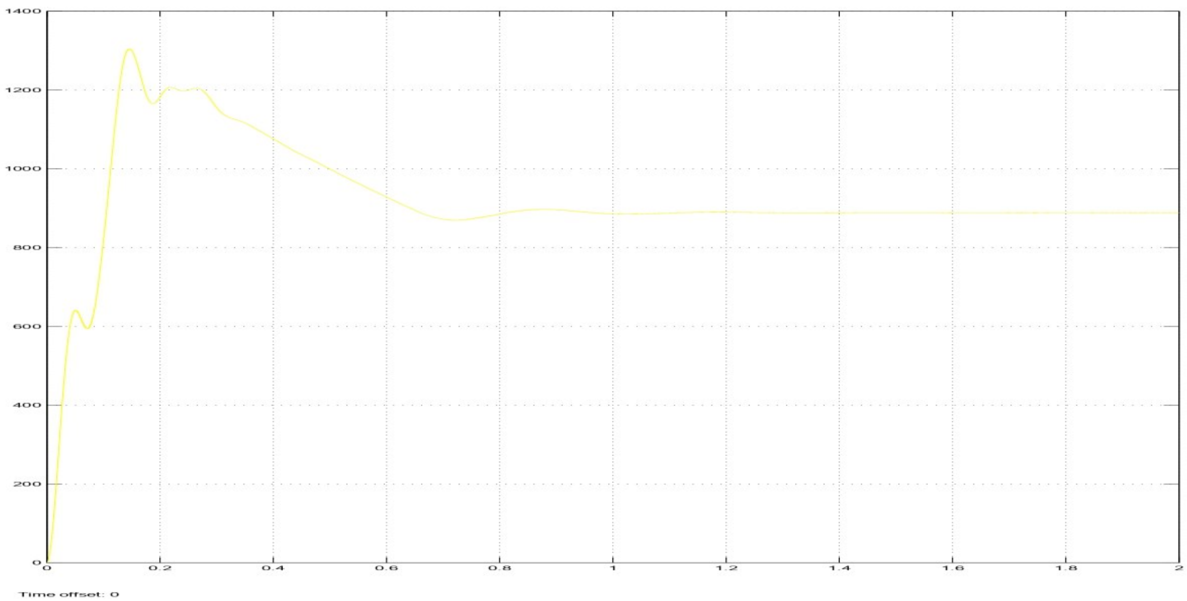

Fig.13 DC-Link Voltage Stability During Converter Operation

This section presents the simulation results of the proposed bidirectional EV charging converter operating under various conditions, as previously described. Each converter is rated at 20 kW with a line-to-line voltage of 400 V and a grid frequency of 50 Hz. The converter can operate at a maximum DC-link voltage of 800 V, resulting in a maximum DC-side current of 32 A. System specifications and parameters are listed in TABLE 1.

TABLE 1. Converter module specifications and system parameters.

Symbols	Descriptions	Values
P	Rated power	20 kW
V_s	Supply voltage from grid	400 Vrms
V_{dc}	DC-link voltage	800 V
f_s	Switching frequency	20 kHz
f_g	Grid frequency	50 Hz
L_g	Filter inductance (grid side)	1.35 mH
C_f	Filter capacitance	50 uF
L_c	Filter inductance (converter side)	0.961 mH
C_{dc}	DC-link capacitance	1000 uF
R_d	Damping resistance	0.01 Ω

A residential building model with a 2500 square-foot (233 m²) apartment, including gas and hot water systems, is used to simulate the proposed system. The total maximum household load is estimated at 36 kWh, accounting for highly inductive appliances like refrigerators, air conditioners, washing machines, dryers, and a 5-ton central AC unit [28].

The small-signal model based on the state-space method is developed in this section. The state transition and input matrices are calculated using the system parameters. The open-loop plant transfer functions for both voltage and current control loops are derived from the state-space model using MATLAB/Simulink. The LCL filter parameters are critical to the plant model, with system stability highly influenced by the filter's inductance and damping resistance values.

In this work, a fuzzy logic controller is employed instead of a traditional PI controller to enhance the robustness and dynamic performance of the system. The fuzzy controller provides better adaptability in nonlinear and variable operating conditions by adjusting control actions based on a set of fuzzy rules, rather than fixed proportional-integral gains.

The influence of series damping resistance R_d on system stability is analyzed. As shown in Figure 16(a), the current control loop maintains a high-frequency attenuation slope of −60 dB/decade. However, the resonance peak frequency increases with higher R_d. Notably, the phase margin becomes negative at 10R_d, indicating near instability. The Nyquist plot in Figure 16(b) confirms the shrinking stability margin as the Nyquist trajectory approaches the (−1, 0) point. The pole-zero map in Figure 16(c) illustrates that system poles remain in the left half-plane until a 10R_d variation. Consequently, as shown in Figure 16(d), the steady-state response becomes oscillatory at high R_d. Similar instability is also observed in the voltage control loop.

These insights help define acceptable parameter limits to avoid unstable operation. The fuzzy-controlled small-signal model is validated against a high-fidelity model in MATLAB/Simulink. The dq-axis current response of the grid-connected inverter is shown in Figure 17.

A single-phase RL residential load is modeled with an initial power demand of 26 kW and 23 kVAR up to $t = 0.15$ s. The load then increases to 38 kW and 36 kVAR until $t = 0.25$ s. During V2H mode, the converter operates in off-grid mode, supplying the load from either the EV battery or solar PV. The initial current demand is 75 A at 400 V (L-L), increasing by about 55 A after the load step. Load parameters are 3 Ω resistance and 9.5 mH inductance.

Figure 17(a) shows the d-axis current through L_g for both the fuzzy-controlled small-signal and high-fidelity models. Up to $t = 0.15$ s, both models closely match, with each converter supplying 38 A. After the load step, the transient responses differ slightly and stabilize around $t = 0.23$ s. Differences in transient response are attributed to the circuit breaker's arc behavior, which isn't initially present due to the contactor being closed.

Importantly, the overshoot in the fuzzy-controlled small-signal model is significantly lower—by about 15 A—compared to the high-fidelity model. This suggests the fuzzy controller offers better damping and reduced overshoot. A similar dynamic response is observed for q-axis current in Figure 17(b), addressing reactive power demand.

Voltage response in Figure 18(a) shows that the fuzzy controller effectively maintains the supply voltage at 230 V (L-N). However, increased reactive power demand causes a slight voltage drop. Figure 18(b) shows that the frequency decreases with rising active power demand. Initially, until $t = 0.15$ s, the frequency reference is about 50.25 Hz, set by the P–f droop control (described in Equations 10 and 11). The controller ensures the converter frequency follows the reference as load demand increases.

Figure 19 illustrates the active and reactive power response from both converters. During V2H mode, the EV battery discharges to meet load demand. The battery performance is shown in Figure 20(a), where the state of charge (SoC) drops faster after $t = 0.15$ s due to higher load. The DC-link voltage remains stable at 800 V, maintained by a pre-charged capacitor. At 26 kW load demand, the battery supplies 38 A.

In Figure 20(b), AC-side voltage and current waveforms during V2H mode show a current of about 50 Arms at 230 V (P-N) with 3% total harmonic distortion (THD). At 38 kW load, the THD drops below 2%, indicating improved power quality at higher loads. However, noticeable output voltage ripple is observed, mainly due to the high switching frequency (20 kHz) and undersized filter capacitor.

The converter also supports charging and V2G (Vehicle-to-Grid) modes. During off-peak hours, the battery is charged; during peak hours, power is returned to the grid. Figure 21 illustrates battery performance in these modes. The EV battery has a nominal voltage of 340 V and a 50 Ah capacity. Charging is performed with a 15 A (0.3C) current until $t = 0.15$ s, providing a 5.5 kW charge rate. The battery reaches full charge in about 3 hours. The fuzzy controller maintains DC-link voltage at 750 V with less than 1% ripple during steady state. After $t = 0.15$ s, the battery discharges to the grid at the same 5.5 kW rate, with the voltage dropping from 370 V to 364 V.

DC-link voltage stabilizes within 0.3 seconds, maintaining acceptable ripple levels (<1%).During charging, the converter draws 38 Arms at 326 V (L-L), and during discharge, it delivers 31 Arms to the grid. Unlike V2H mode, AC voltage and current ripples are minimal, indicating that the fuzzy controller gain tuning and switching frequency are well-suited for these operations. Throughout charging and V2G modes, the AC current THD remains below 2%, ensuring high power quality.

V. Conclusion

This paper presents a comprehensive analysis of an integrated electric vehicle (EV) charging station designed for residential applications, focusing on system design, control strategy, and performance validation. The proposed system incorporates a grid-interfacing inverter capable of supporting energy storage, solar PV integration, and acting as a buffer power supply to enhance energy flexibility and resilience.

To control the system dynamics, a fuzzy logic controller is employed in place of a conventional PI controller. The fuzzy controller significantly improves system adaptability under varying operating conditions by dynamically adjusting control actions based on linguistic rules, thereby enhancing both transient and steady-state performance. Compared to the high-fidelity (HiFi) model, the fuzzy-controlled system achieves a performance error of only 0.46% under normal conditions. During dynamic load transitions, which take approximately 1.5 seconds to stabilize, the performance error increases moderately to 5–10%. This still remains within acceptable limits, showing the effectiveness of the fuzzy controller in handling nonlinear behavior and load disturbances.

In V2H mode, the system maintains a total harmonic distortion (THD) of approximately 5% while supplying an RL load. During charging and V2G operations, the fuzzy controller effectively regulates the DC-link voltage to around 750 V with less than 1% ripple in steady-state conditions. At $t = 0.15$ s, the EV battery begins discharging to the grid at a rate of 5.5 kW, with the battery voltage decreasing from 370 V to 364 V. The DC-link voltage stabilizes within 0.3 seconds, confirming the enhanced response and robustness of the fuzzy logic-based control.

Reference:

[1] (Apr. 23, 2023). *Brussles Transit Company STIB Will Replace 411 Diesel Buses by 2030*. Accessed: Feb. 28, 2023. [Online]. Available: https://www.brusselstimes.com/219102/brussels-transit-company-stibwill- replace-411-diesel-buses-by-2030
[2] *De LIJN to Buy up to 1,250 Electric Buses Within 6 Years*. Accessed: Feb. 28, 2023. [Online]. Available: https://www.electrive.com/ 2022/03/31/de-lijn-to-procure-up-to-1250-electric-buses-within-sixyears/
[3] M. Molliere. (Mar. 2022). *E-Vans: Cheaper, Greener and in Demand*. Accessed: Feb. 28, 2023. [Online]. Available: https://www. transportenvironment.org/wp-content/uploads/2022/03/2022_03_van_ TCO_report-1.pdf
[4] J. Conzade, F. Nägele, S. Ramanathan, and P. Schaufuss. (Nov. 2022). *Europe's EV Opportunity—And the Charging Infrastructure Needed to Meet it*. Mckinsey & Company. Accessed: Feb. 28, 2023. [Online]. Available: https://www.mckinsey.com/industries/automotive-andassembly/ our-insights/europes-ev-opportunity-and-the-charginginfrastructure- needed-to-meet-it
[5] A. Ahmad, M. Khalid, Z. Ullah, N. Ahmad, M. Aljaidi, F. A. Malik, and U. Manzoor, ''Electric vehicle charging modes, technologies and applications of smart charging,'' *Energies*, vol. 15, no. 24, p. 9471, Dec. 2022.
[6] J. Johnson, T. Berg, B. Anderson, and B. Wright, ''Review of electric vehicle charger cybersecurity vulnerabilities, potential impacts, and defenses,'' *Energies*, vol. 15, no. 11, p. 3931, 3931.
[7] *Solar Energy Deployment in EU 2030: Global Energy Crisis Series*. ECO Green Energy. Accessed: Mar. 12, 2023. [Online]. Available: https://www.eco-greenenergy.com/solar-energy-deployment-in-eu-2030- global-energy-crisis/
[8] *New Analysis Reveals Over 1 Million European Homes are Solar Battery- Powered*. Solar Power Europe. Accessed: Mar. 12, 2023. [Online]. Available: https://www.solarpowereurope.org/press-releases/newanalysis- reveals-over-1-million-european-homes-are-solar-batterypowered
[9] (Jul. 2022). *Electric Cars as Buffer Storage for Solar Power: Infineon and Delta Enable Bidirectional Charging at Home*. Accessed: Mar. 12, 2023. [Online]. Available: https://www.infineon.com/ cms/en/aboutinfineon/ press/press-releases/2022/INFIPC202207-105.html
[10] *Fast EV Charging*. Infineon (DC Wallbox). Accessed: Mar. 12, 2023. [Online]. Available: https://www.infineon.com/cms/en/ applications/industrial/ev-charging/dc-wallbox/

[11] M. A. H. Rafi and J. Bauman, ‘‘A comprehensive review of DC fastcharging stations with energy storage: Architectures, power converters, and analysis,’’ *IEEE Trans. Transport. Electrific.*, vol. 7, no. 2, pp. 345–368, Jun. 2021.
[12] G. Rituraj, G. R. C. Mouli, and P. Bauer, ‘‘A comprehensive review on offgrid and hybrid charging systems for electric vehicles,’’ *IEEE Open J. Ind. Electron. Soc.*, vol. 3, pp. 203–222, 2022.
[13] I. Worighi, T. Geury, M. El Baghdadi, J. Van Mierlo, O. Hegazy, and A. Maach, ‘‘Optimal design of hybrid PV-battery system in residential buildings: End-user economics, and PV penetration,’’ *Appl. Sci.*, vol. 9, no. 5, p. 1022, 2019, doi: 10.3390/app9051022.
[14] (Jul. 2022). *ADS-TEC Energy White Paper Published in Businesswire*. Accessed: Mar. 12, 2023. [Online]. Available: https://www. businesswire.com/news/home/20220706005129/en/New-Research-Shows-How-Ultra-Fast-Battery-Buffered-EV-Charging-Technology- Can-Meet-Increasing-Demands-and-Save-Charge-Network-Operators- Up-to-30-in-TCO.
[15] D. Huber, Q. De Clerck, C. De Cauwer, N. Sapountzoglou, T. Coosemans, and M. Messagie, ‘‘Vehicle to grid impacts on the total cost of ownership for electric vehicle drivers,’’*World Electric Vehicle J.*, vol. 12, no. 4, p. 236, Nov. 2021.
[16] G. R. C. Mouli, J. Kaptein, P. Bauer, and M. Zeman, ‘‘Implementation of dynamic charging and V2G using chademo and CCS/COMBO DC charging standard,’’ in *Proc. IEEE Transp. Electrific. Conf. Expo (ITEC)*, Dearborn, MI, USA, Jun. 2016, pp. 1–6.
[17] S. Jaman, B. Verbrugge, O. H. Garcia, M. Abdel-Monem, B. Oliver, T. Geury, and O. Hegazy, ‘‘Development and validation of V2G technology for electric vehicle chargers using combo CCS type 2 connector standards,’’ *Energies*, vol. 15, no. 19, p. 7364, 2022.
[18] *Off Grid Solar System For Home With Battery Backup, 2023*. Kenbrook Solar. Accessed: Mar. 12, 2023. [Online]. Available: https://kenbrooksolar.com/solar-power-plants/1kw-2kw-5kw-10kwoff-grid-solar-power-plants
[19] J. Svarc. (Mar. 10, 2023). *Home Solar EV Charging*. Clean Energy Reviews. Accessed: Jul. 11, 2023. [Online]. Available: https://www. cleanenergyreviews.info/blog/solar-ev-charging
[20] *What is the Average Electricity and Gas Consumption in the Brussels Region*. Sibelga Energguide. [Online]. Available: https://www.energuide.be/en/questions-answers/what-is-the-averageelectricity-and-gas-consumption-in-the-brussels-region/273/